

SUPPLEMENTAL MATERIAL

Supporting information of this manuscript includes eleven figures and seven tables:

Figure S1. Sequence alignment of Arabidopsis ADHs

Figure S2. Structural superposition of NAD⁺-GSNOR monomers

Figure S3. Coordination geometry of structural zinc ion in Arabidopsis ADHs

Figure S4. Coordination geometry of catalytic zinc ion in Arabidopsis ADHs

Figure S5. ADH1 and GSNOR structural superpositions

Figure S6. Sequence alignment to highlight cysteine conservation and catalytic-related residues in ADH1 and GSNOR.

Figure S7. Determination of pH optimum for ADH1 and GSNOR catalysis

Figure S8. Solvent excluded surface of the internal cavity calculated for ADH1 and GSNOR structures

Figure S9. Structural stability of GSNOR in response to thiol-modifying agents

Figure S10. Structural stability of ADH1 in response to thiol-modifying agents

Figure S11. Circular dichroism (CD) spectra of ADH1 and GSNOR

Tables S1. Root mean square deviation (RMSD) values in Å, obtained from the superpositions of ADH1 and GSNOR monomers.

Table S2. Root mean square deviation (RMSD) values in Å, obtained from the superpositions of ADH1 and GSNOR dimers

Table S3. Minimum, maximum, average root mean square deviation (RMSD) values and standard deviations (SD), obtained from the superpositions of ADH1 and GSNOR monomers and dimers.

Table S4. Hydrogen bond interactions between the cofactor (NAD⁺ or NADH) and the protein residues in ADH structures.

Table S5. Accessibility surface area (ASA) values of cysteine residues and their Sγ atoms in ADHs structures.

Table S6. Secondary structure estimations for ADH1 and GSNOR before and after treatment with MMTS or H₂O₂.

Table S7. Data collection and refinement statistics of ADHs structures.

Figure S1

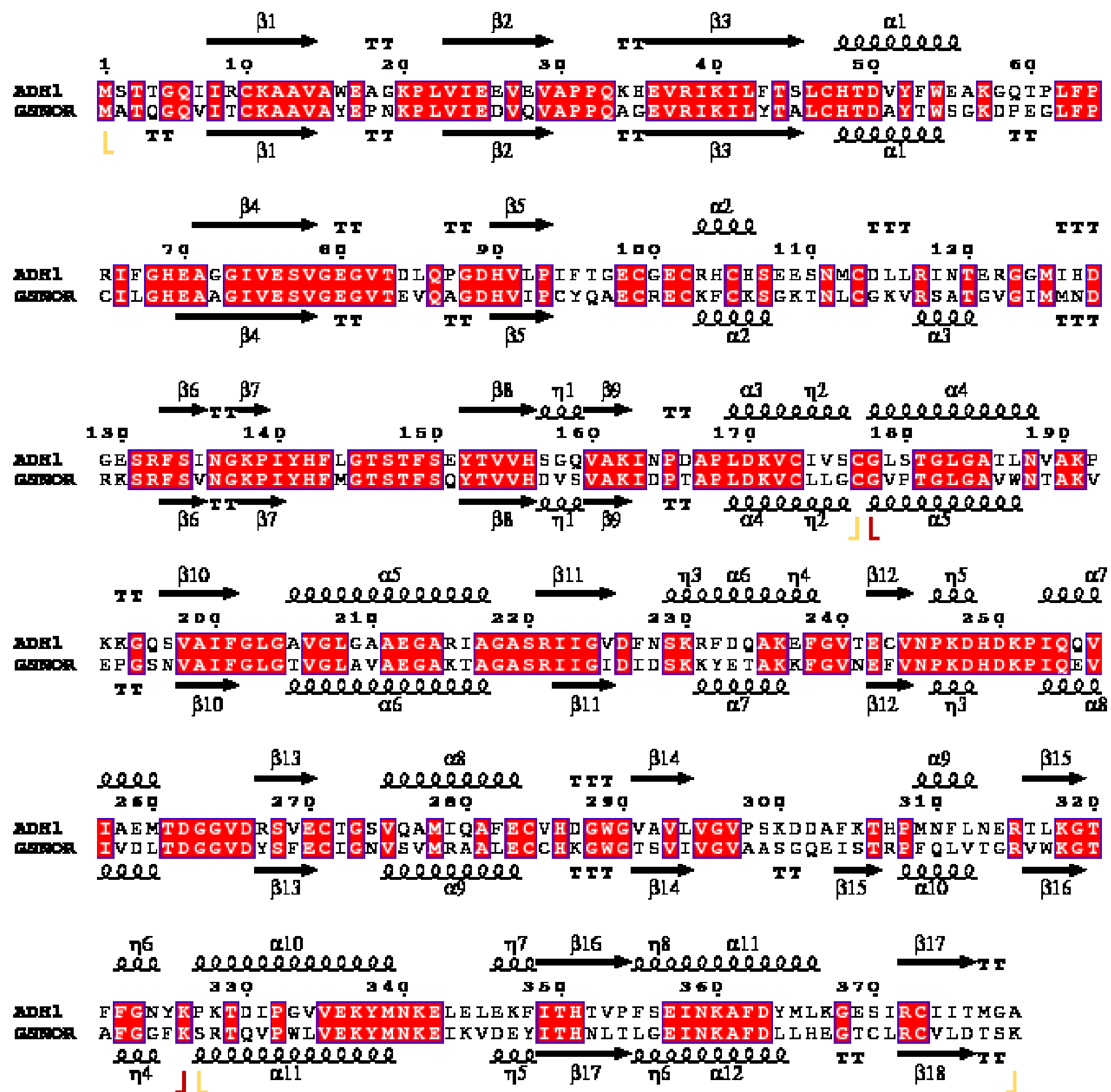


Figure S1. Sequence alignment of *Arabidopsis* ADHs

The alignment was performed as described in (Mattioli *et al.*, 2022) using the sequence and the structure of *Arabidopsis thaliana* ADH1 (PDB ID: 4RQU) and GSNOR (PDB ID: 4JJ1). The conserved residues are shown in red background; blue boxes represent conserved amino acid stretches (>70%). Residues with similar physico-chemical properties are indicated in red. The following symbols “L” and “J” were used to indicate the start and end of the catalytic domain (yellow) and the cofactor binding domain (dark red), respectively. α-helices, β-strands and 3₁₀-helices are marked with α, β, η respectively. β-turns and α-turns are represented by TT and TTT, respectively. ADH1 and GSNOR share ~59% sequence identity and exhibit a nearly complete conservation of secondary structures except for a small α-helix (residues 117-120), a short β-strand (residues 304-306), and two β-turns (residues 300-301 and 368-369), found only in GSNOR. The start and end

Figure S2

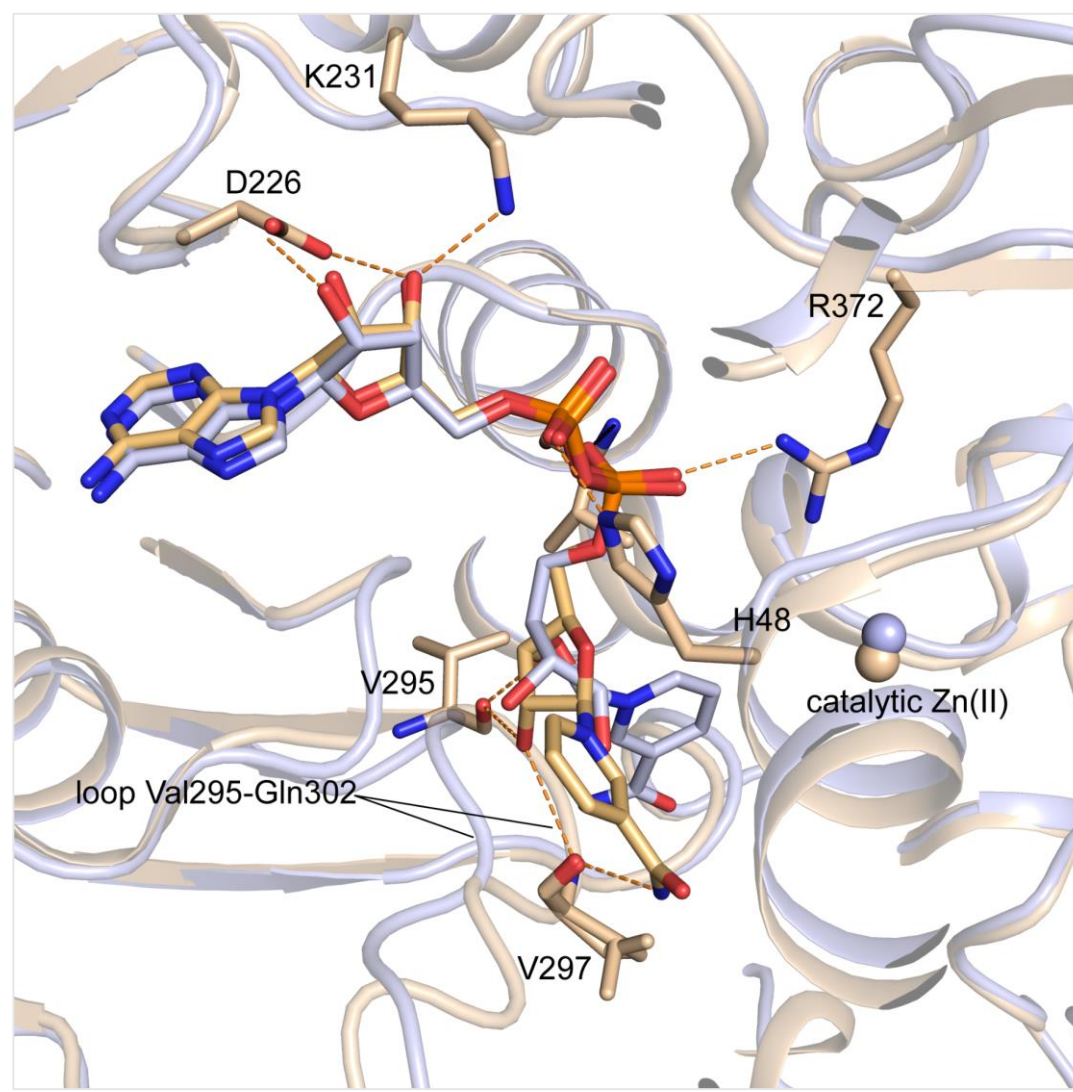


Figure S2. Structural superimposition of NAD⁺-GSNOR monomers.

Superimposition of NAD⁺ and the cofactor-binding site in GSNOR monomers (PDB ID 4JJI). Chain A (light blue) shows a nicotinamide moiety conformation similar to the structures of other available ADHs, while in chain B (wheat) the nicotinamide moiety is rotated of about 90°. In addition, the loop Val295-Gln302, which is located at the entrance of the active site, shows a different conformation in chain B with respect to chain A. Protein chain is represented as cartoon, NAD⁺ and residues as sticks and the catalytic Zn(II) as sphere. The interactions between protein residues and NAD⁺ of chain B are indicated and the corresponding distances values are reported in Table S4.

Figure S3

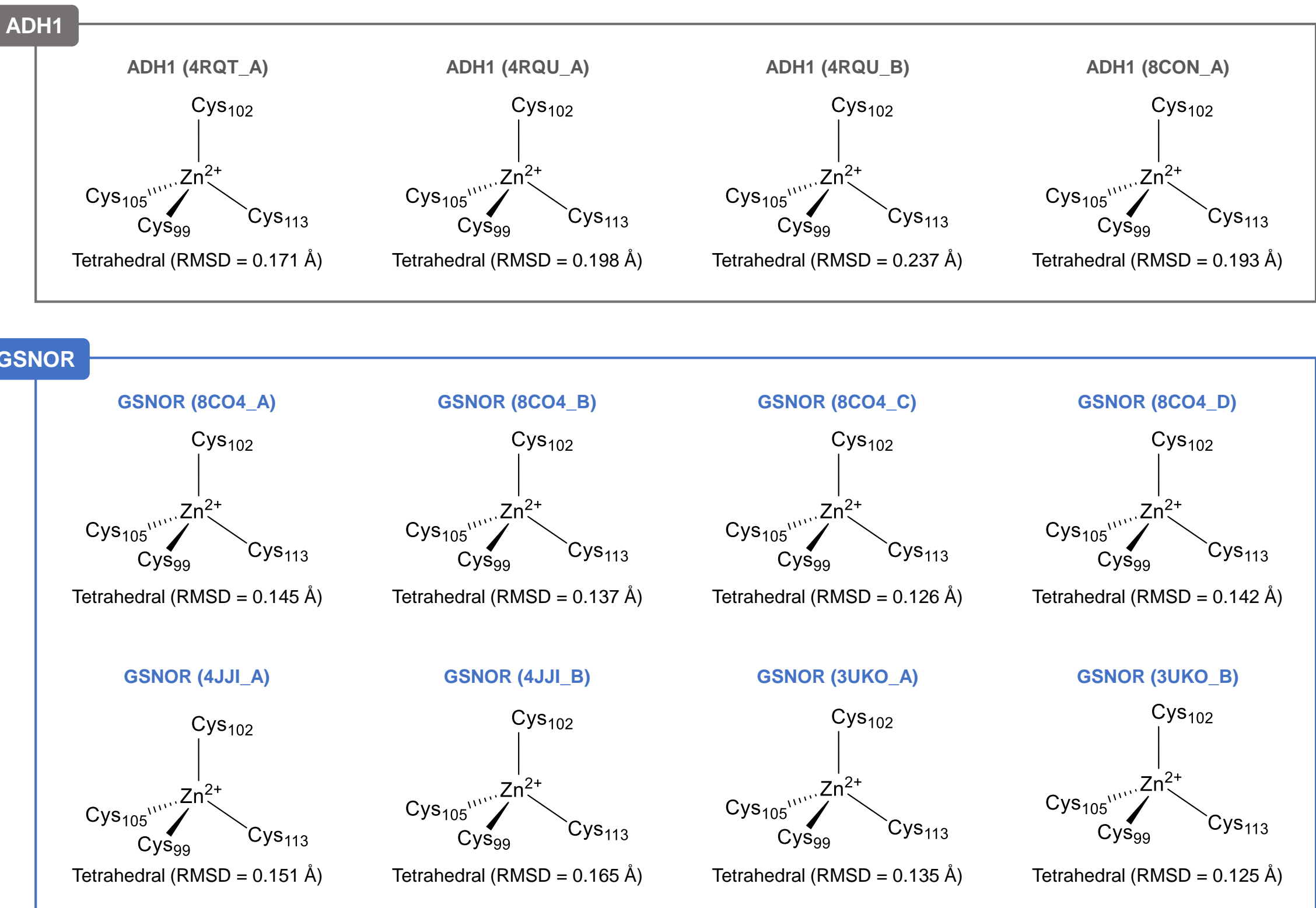


Figure S3. Coordination geometry of structural zinc ion in ADHs.

Schemes of the coordination geometries of the structural zinc ions found in ADH1 and GSNOR crystal structures. The RMSD from the ideal geometry has been calculated using the UCSF Chimera “Metal Geometry” tool. Legend to PDB IDs for ADH1: 4RQT, apo/acetate-form; 4RQU, NAD⁺-form; 8CON, NADH-form. Legend to PDB IDs for GSNOR: 8CO4, apo-form; 4JJI, NAD⁺-form; 3UKO, NADH-form. The letter indicates the structural chain.

Figure S4

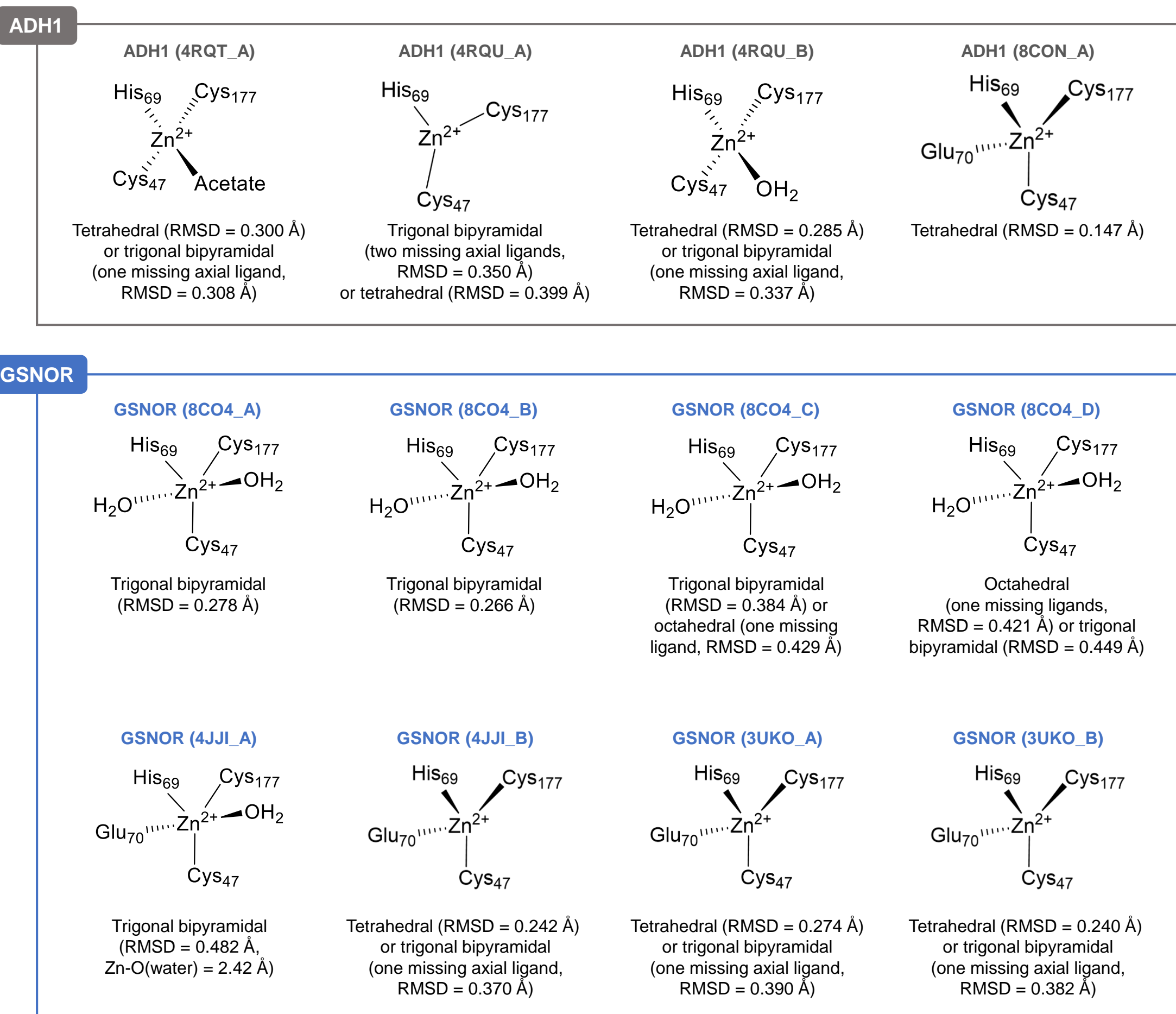
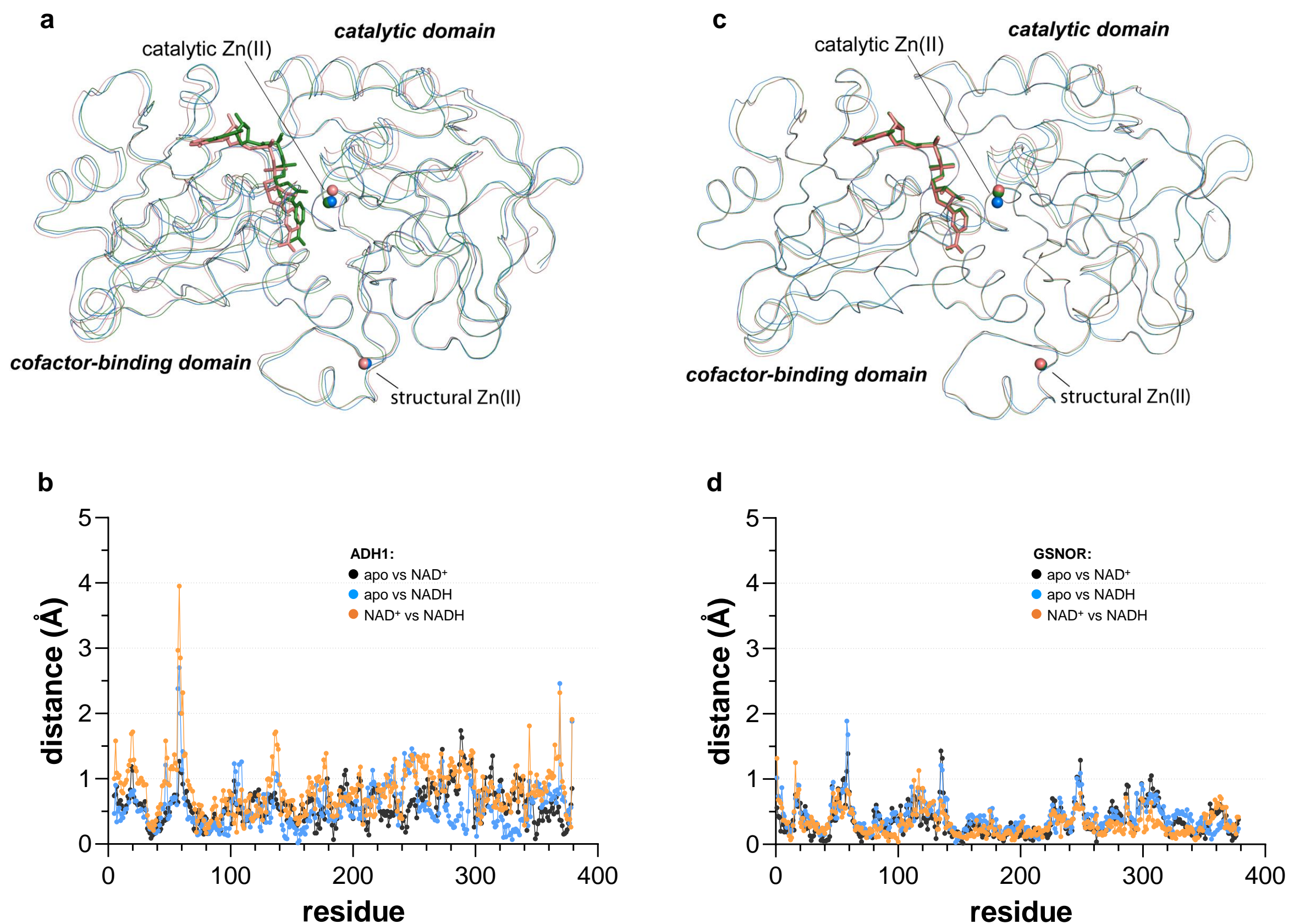


Figure S4. Coordination geometry of catalytic zinc ion in ADHs.

Schemes of the coordination geometries of the catalytic zinc ions found in ADH1 and GSNOR crystal structures. The RMSD from the ideal geometry has been calculated using the UCSF Chimera "Metal Geometry" tool. Legend to PDB IDs for ADH1: 4RQT, apo/acetate-form; 4RQU, NAD⁺-form; 8CON, NADH-form. Legend to PDB IDs for GSNOR: 8CO4, apo-form; 4JJI, NAD⁺-form; 3UKO, NADH-form. The letter indicates the structural chain.

Figure S5**Figure S5. ADH1 and GSNOR structural superimpositions.**

Superimposition of ADH1 (a) and GSNOR (c) monomers. The protein backbone is reported as ribbon colored in blue, dark green and salmon for apo-, NAD^+ - and NADH-structures, respectively. The cofactor and zinc ions are reported as sticks and spheres, respectively, colored with the same color scheme. RMSD values per residue obtained from the C_α atoms superimposition of monomers of ADH1 (b) and GSNOR (d).

Figure S6

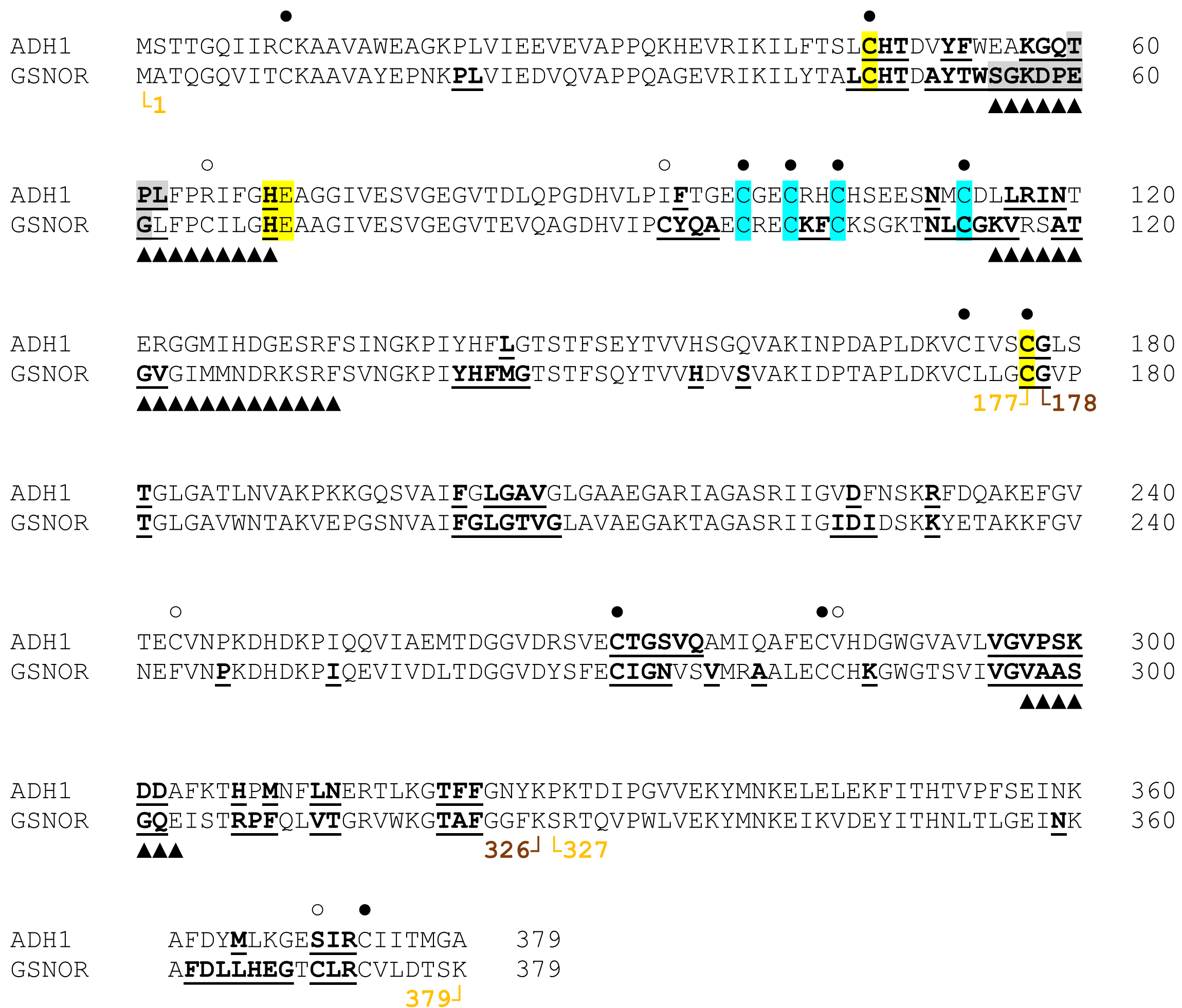


Figure S6. Sequence alignment to highlight cysteine conservation and catalytic-related residues in ADH1 and GSNOR.

Conserved and unique cysteine residues are indicated by closed and open circles, respectively. The selection of residues found in the catalytic cavity of both ADH1 and GSNOR was based on their presence in the active site for more than the 50% of the available structures (at least 3 for ADH1 and 5 for GSNOR). These residues are highlighted in bold and underlined.. Non-conserved regions that delimit the entrance to the catalytic cavity and form the cavity itself (loop 55-69, and stretches 115-132 and 297-303) are indicated by closed triangles. The distinctive sequences in the active site for alcohol dehydrogenases capable to process ethanol (ADH1) or to degrade GSNO (GSNOR) are shown in gray (Bui *et al.*, 2019). Residues involved in the binding of the catalytic and structural zinc ions are highlighted in yellow and cyan, respectively. The following symbols “L” and “J” were used to indicate the start and end of the catalytic domain (yellow) and the cofactor binding domain (dark red), respectively.

Figure S7

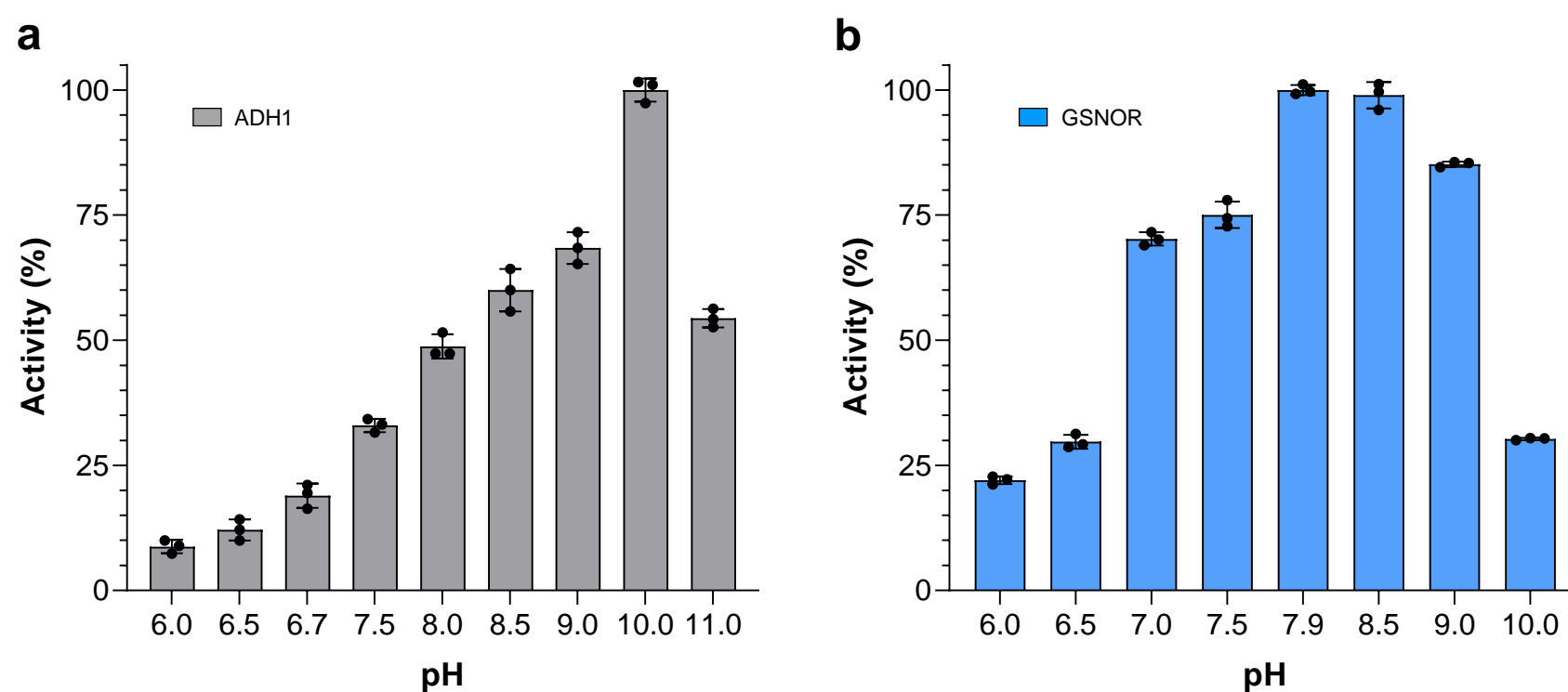
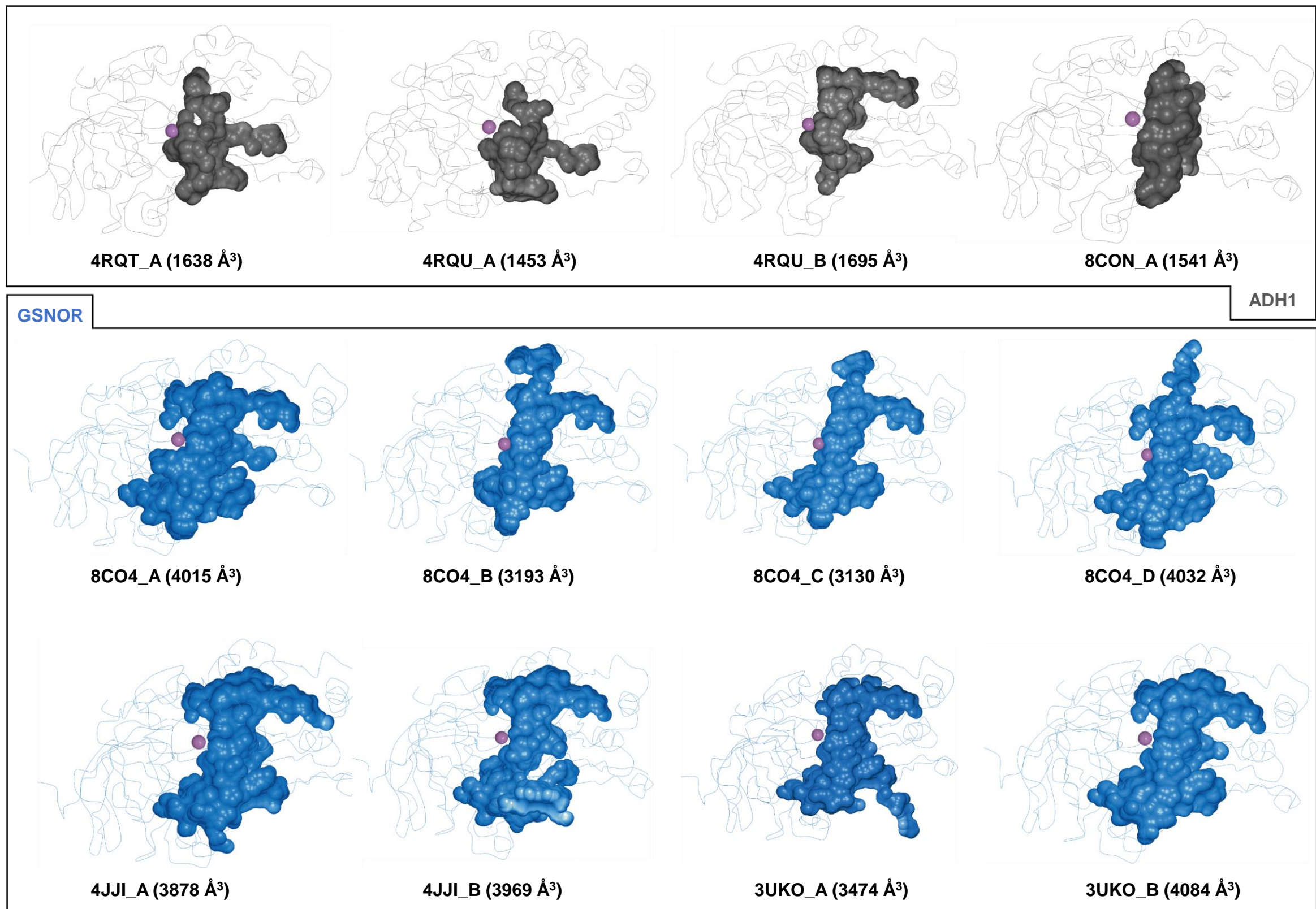
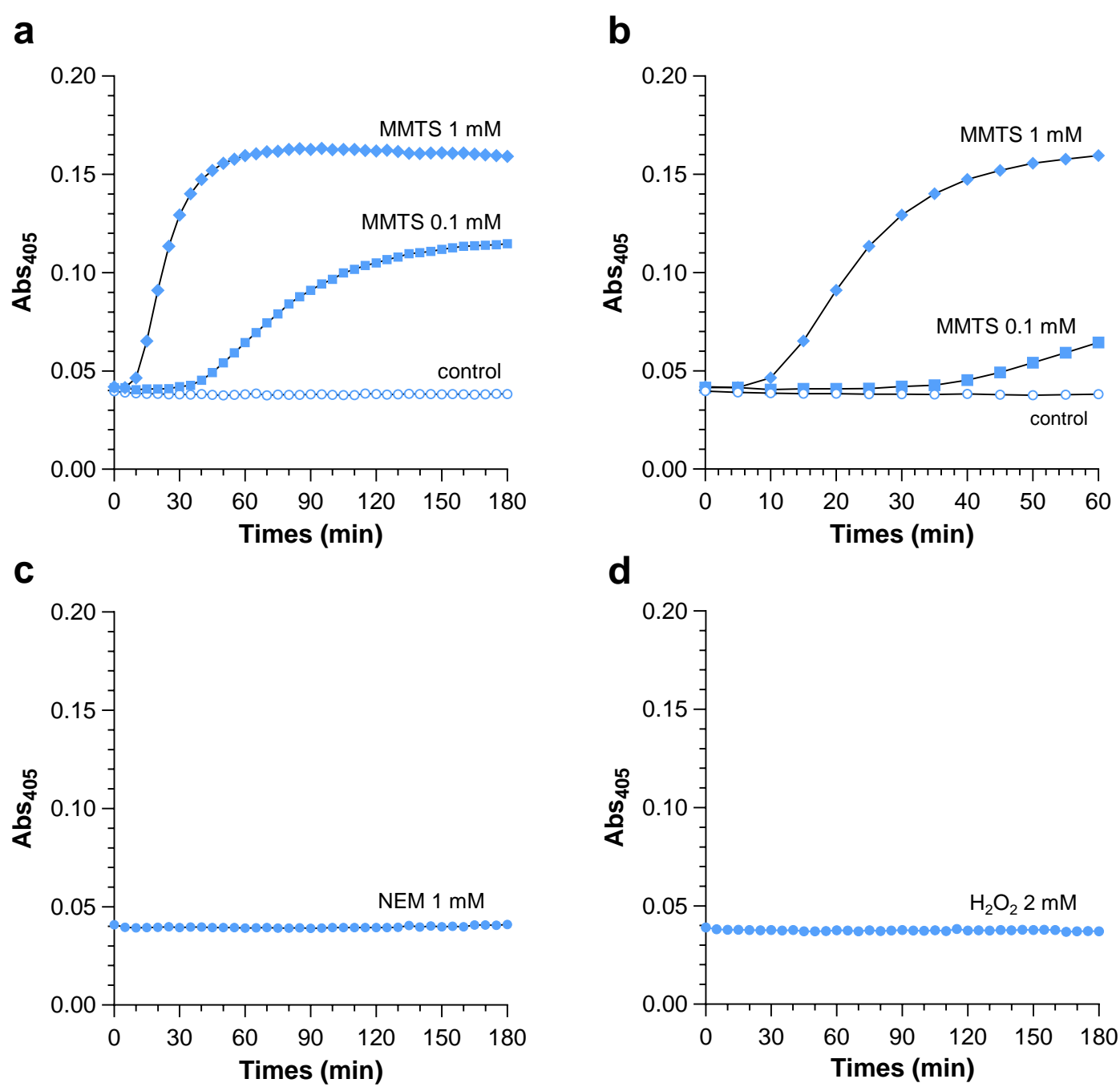


Figure S7. Determination of pH optimum for ADH1 and GSNOR catalysis.

(a) A plot of pH value versus the relative activity of ADH1 (grey bars). Values are represented as percentage of the maximal activity measured at pH 10. (b) A plot of pH value versus the relative activity of GSNOR (light blue bars). Values are represented as percentage of the maximal activity measured at pH 7.9. For both panels, data are represented as mean \pm SD ($n = 3$).

Figure S8**Figure S8. Solvent excluded surface of the internal cavity calculated for ADH1 and GSNOR structures.**

Solvent-excluded surfaces of the catalytic cavities of ADH1 (top panel, gray) and GSNOR (bottom panel, light blue). The backbone of the protein is shown for reference as a thin ribbon. The catalytic zinc ion is represented by a purple sphere. The NAD⁺/NADH cofactors have been removed in order to compare different structures. Legend to PDB IDs for ADH1: 4RQT, apo/acetate-form; 4RQU, NAD⁺-form; 8CON, NADH-form. Legend to PDB IDs for GSNOR: 8CO4, apo-form; 4JJI, NAD⁺-form; 3UKO, NADH-form. The letter indicates the structural chain.

Figure S9**Figure S9. Structural stability of GSNOR in response to thiol-modifying agents.**

(a) GSNOR was incubated up to 180 min under control conditions (control) or in the presence of 0.1 or 1 mM MMTS. (b) GSNOR was incubated as in panel A and the data are represented up to 60 min. (c) GSNOR was incubated up to 180 min in the presence of 1 mM NEM. (d) GSNOR was incubated up to 180 min in the presence of 2 mM H₂O₂. For all panels, protein stability was evaluated following the turbidity increase at 405 nm as a proxy of protein misfolding. Data are represented as mean of three independent biological replicates (n = 3).

Figure S10

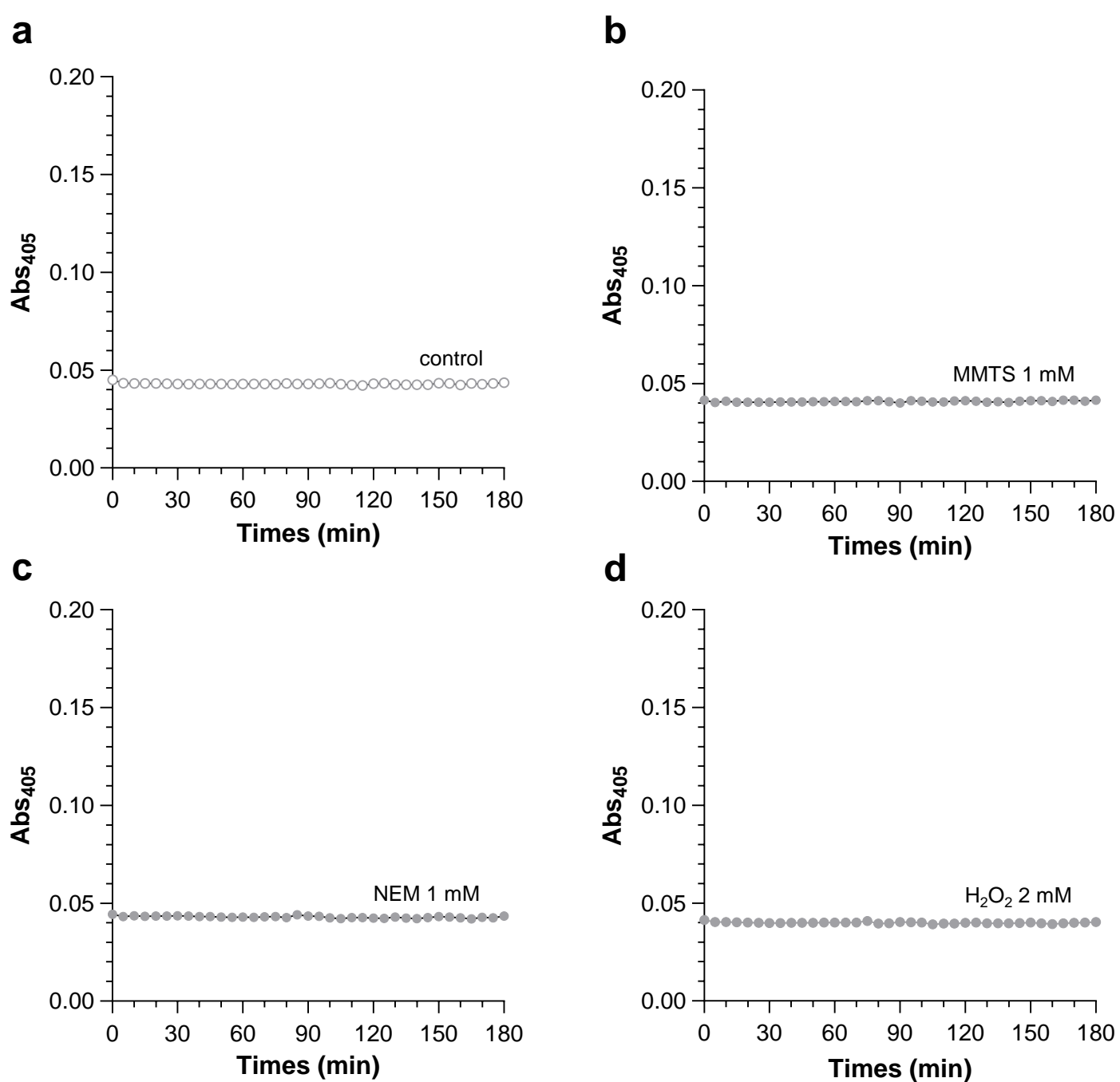


Figure S10. Structural stability of ADH1 in response to thiol-modifying agents.

ADH1 was incubated up to 180 min under control conditions (a, control), in the presence of 1 mM MMTS (b), 1 mM NEM (c), or 2 mM H_2O_2 (d). For all panels, protein stability was evaluated following the turbidity increase at 405 nm as a proxy of protein misfolding. Data are represented as mean of three independent biological replicates ($n = 3$).

Figure S11

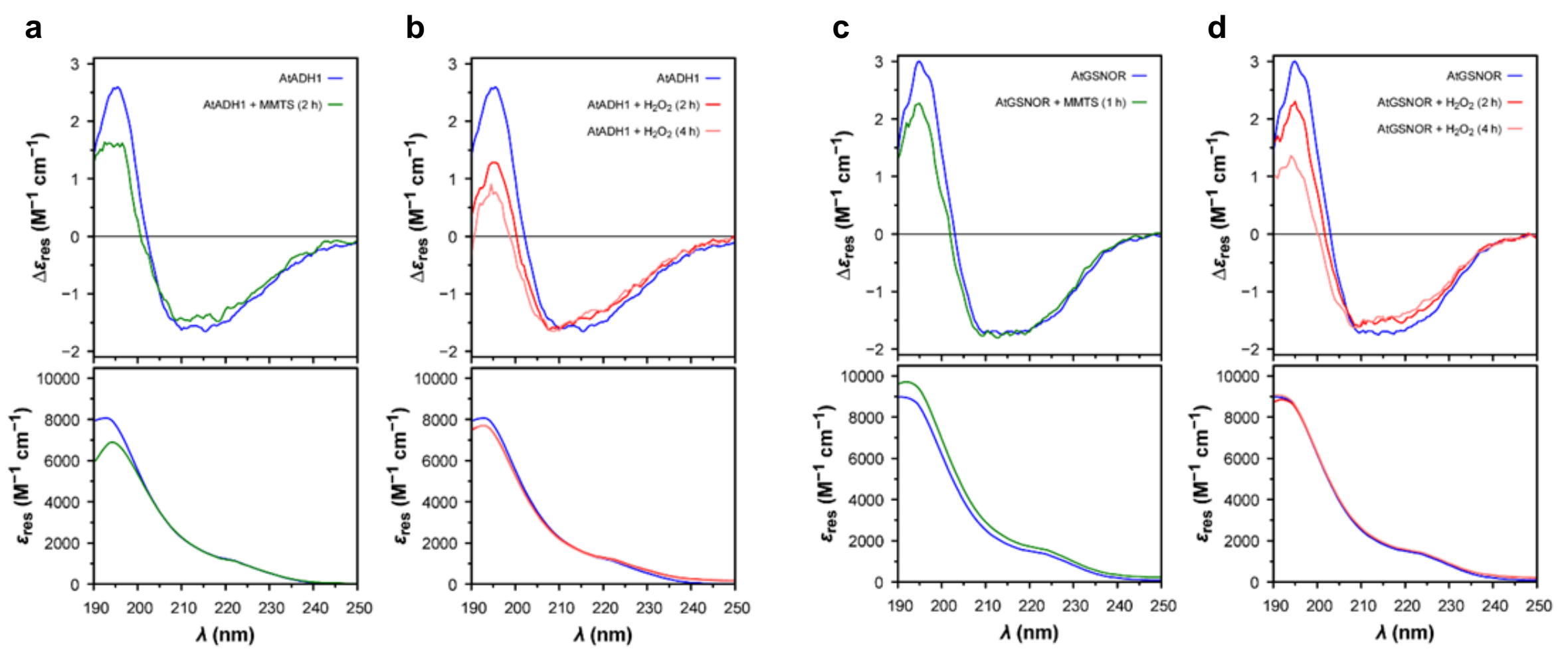


Figure S11. Circular dichroism (CD) spectra of ADH1 and GSNOR.

(a) ADH1 (10 μM) before and after incubation with MMTS (0.1 mM) for 2 h. (b) ADH1 (10 μM) before and after incubation with H₂O₂ (2 mM) for 2 and 4 h. (c) GSNOR (10 μM) before and after incubation with MMTS (0.1 mM) for 1 h. (d) GSNOR (10 μM) before and after incubation with H₂O₂ (2 mM) for 2 and 4 h.

Table S1. Root mean square deviation (RMSD) values in Å, obtained from the superimpositions of ADH1 and GSNOR monomers.

		RMSD (Å)											
Protein		Apo-ADH1	NAD-ADH1		NADH-ADH1†	Apo-GSNOR†				NAD-GSNOR		NADH-GSNOR	
	PDB ID_chain	4RQT_A	4RQU_A‡	4RQU_B	8CON_A	8CO4_A	8CO4_B	8CO4_C	8CO4_D	4JJI_A	4JJI_B§	3UKO_A	3UKO_B
Apo-ADH1	4RQT_A	-	0.48	0.66	0.67	1.25	1.30	1.32	1.26	1.10	1.27	1.06	1.18
NAD-ADH1	4RQU_A ²		-	0.67	0.73	1.43	1.52	1.51	1.46	1.22	1.43	1.16	1.32
	4RQU_B			-	0.95	1.10	1.11	1.12	1.01	0.99	1.26	1.07	1.17
NADH-ADH1	8CON_A				-	1.20	1.32	1.32	1.28	0.95	1.20	0.93	1.11
Apo-GSNOR	8CO4_A					-	0.38	0.40	0.47	0.43	0.68	0.69	0.47
	8CO4_B						-	0.35	0.45	0.48	0.77	0.62	0.56
	8CO4_C							-	0.49	0.56	0.80	0.70	0.62
	8CO4_D								-	0.59	0.98	0.82	0.75
NAD-GSNOR	4JJI_A									-	0.67	0.43	0.38
	4JJI_B§										-	0.77	0.43
NADH-GSNOR	3UKO_A										-		0.56
	3UKO_B												-

†These structures were determined in this study.

‡This monomer was solved without the cofactor.

§This monomer shows a different conformation of the nicotinamide moiety of NAD⁺.

Table S2. Root mean square deviation (RMSD) values in Å, obtained from the superimpositions of ADH1 and GSNOR dimers.

		RMSD (Å)						
Protein	PDB ID_chains	Apo-ADH1	NAD-ADH1	NADH-ADH1 [†]	Apo-GSNOR [†]		NAD-GSNOR	NADH-GSNOR
Apo-ADH1	4RQT_AA ^{sym}	-	1.10	0.83	2.30	2.43	2.06	1.90
NAD-ADH1	4RQU_AB [‡]		-	1.16	2.12	2.06	1.97	1.82
NADH-ADH1	8CON_AA ^{sym}			-	1.98	2.06	1.68	1.58
Apo-GSNOR	8CO4_AB				-	0.52	0.86	0.87
	8CO4_CD					-	1.09	1.07
NAD-GSNOR	4JJI_AB [§]						-	0.45
NADH-GSNOR	3UKO_AB							-

[†]These structures were determined in this study.

[‡]Chain A in this dimer was solved without the cofactor.

[§]Chain B in this dimer shows a different conformation of the nicotinamide moiety of NAD⁺.

Table S3. Minimum, maximum, average root mean square deviation (RMSD) values and standard deviations (SD), obtained from the superimpositions of ADH1 and GSNOR monomers and dimers.

	Minimum RMSD (Å)	Maximum RMSD (Å)	$\langle \text{RMSD} \rangle$ (Å)	SD (Å)
Monomers				
ADH1 vs. ADH1	0.48	0.95	0.69	0.15
GSNOR vs. GSNOR	0.35	0.98	0.58	0.16
ADH1 vs. GSNOR	0.93	1.52	1.22	0.16
Dimers				
ADH1 vs. ADH1	0.83	1.16	1.13	0.18
GSNOR vs. GSNOR	0.45	1.09	0.81	0.27
ADH1 vs. GSNOR	1.58	2.43	2.00	0.24

Table S4. Hydrogen bond interactions between the cofactor (NAD⁺ or NADH) and the protein residues in ADH structures. Residues in bold, correspond to non-conserved amino acids between ADH1 and GSNOR. Only interactions at a distance ≤ 3.6 Å are considered.

ADH1					GSNOR							
4RQU (NAD ⁺)			8CON (NADH)		4JJ1 (NAD ⁺)				3UKO (NADH)			
Residue (atom)	Atom	Dist. (Å)	Atom	Dist. (Å)	Residue (atom)	Atom	Dist. (Å)	Atom	Dist. (Å)	Atom	Dist. (Å)	
Chain B			Chain A		Chain A			Chain B			Chain A	Chain B
Asp226 (OD1)	O2B	2.62	O2B	2.61	Asp226 (OD1)	O2B	2.38	O2B	2.59	O2B	2.57	2.63
Asp226 (OD2)	O3B	3.00	O3B	2.58	Asp226 (OD2)	O3B	2.63	O3B	2.82	O3B	2.59	2.71
Arg231(NH1/NE)	O3B	2.56	O3B	3.31	Lys231 (NZ)	-	-	O3B	2.79	O3B	2.97	2.68
His48 (N/NE)	O1N	3.46	O1A	3.12	His48 (ND1/NE2)	-	-	O1A	2.58	O1A	3.02	2.46
Ala205(N)	O2N	3.15	O2N	3.30	Thr205 (N)	O2N	3.06	-	-	O2N	3.23	3.19
Val206(N)	O2N	2.82	O2N	3.02	Val206 (N)	O2N	3.02	O2N	3.00	O2N	2.97	2.97
Arg372(NH1)	O1N	3.32	/	/	Arg372 (NH1)	O1N	3.07	O1N	2.91	O1N	3.12	3.07
Arg372(NH2)	O1N	3.37	/	/	Arg372 (NH2)	-	-	-	-	-	-	-
Thr272(O)	O3D	3.07	/	/	Ile272 (O)	O3D	2.98	-	-	O3D	2.82	2.82
Thr49(OG1)	O2D	2.92	/	/	Thr49 (OG1)	-	-	-	-	-	-	-
Val297(N)	O3D	3.60	O3D	2.99	Val297 (N)	O3D	3.20	-	-	O3D	3.12	3.06
Val297(O)	-	-	-	-	Val297 (O)	-	-	O2D	3.33	-	-	-
Val297(O)	-	-	-	-	Val297 (O)	-	-	N7N	2.94	-	-	-
Val295(O)	N7N	3.22	N7N	2.86	Val295 (O)	N7N	2.87	-	-	N7N	2.90	2.89
Val295(O)	-	-	-	-	Val295 (O)	-	-	O2D	3.36	-	-	-
Val295(O)	-	-	-	-	Val295 (O)	-	-	O3D	2.82	-	-	-
Thr320(O)	/	/	N7N	3.07	Thr320 (O)	N7N	2.79	-	-	N7N	2.97	2.71
Phe322(N)	O7N	2.82	O7N	2.76	Phe322 (N)	O7N	2.87	-	-	O7N	2.80	2.74
Phe95	-	-	-	-	Tyr95 (OH)	O7N	3.40	-	-	O7N	3.71	3.10

Table S5. Accessibility surface area (ASA) values of cysteine residues and their $\text{S}\gamma$ atoms in ADHs structures. Cysteines highlighted in green and blue are those involved in the coordination of structural and catalytic zinc ions, respectively. The values in bold refer to the most accessible cysteines in the apo structures of both enzymes.

ADH1					GSNOR							
Apo (4RQT)	NAD ⁺ (4RQU)	NAD ⁺ (4RQU)	NADH (8CON)		Apo (8CO4)				NAD ⁺ (4JJ1)		NADH (3UKO)	
Chain A	Chain A [†]	Chain B	Chain A		Chain A	Chain B	Chain C	Chain D	Chain A	Chain B [‡]	Chain A	Chain B
Cys	ASA _{tot} (ASA _{Sy}) (\AA^2)				ASA _{tot} (ASA _{Sy}) (\AA^2)							
10	4.1(0.0)	5.6(0.0)	3.5(0.0)	5.3(0.0)	5.2(0.0)	4.7(0.0)	6.3(0.0)	5.9(0.0)	4.3(0.0)	5.6(0.0)	4.1(0.0)	5.3(0.0)
47	0.8(0.8)	0.1(0.1)	0.0(0.0)	2.7(2.2)	9.7(9.7)	10.4(10.0)	10.9(10.9)	9.1(9.1)	0.8(0.4)	6.4(5.9)	3.0(1.9)	1.8(0.7)
65	/	/	/	/	1.6(0.7)	2.2(1.5)	1.0(0.7)	1.3(0.6)	1.6(1.0)	1.0(0.6)	1.8(1.1)	0.9(0.7)
94	/	/	/	/	1.7(0.4) [§]	1.2(0.0) [§]	1.7(0.4) [§]	0.9(0.2) [§]	1.7(0.0)	1.3(0.4)	1.9(0.0)	0.8(0.1)
99	35.8(4.0)	28.4(2.3)	35.3(3.9)	34.3(3.1)	9.9(0.4)	6.2(0.0)	8.1(0.2)	11.8(0.5)	14.2(0.9)	13.8(0.1)	15.0(1.2)	14.0(0.1)
102	21.6(0.0)	20.5(0.0)	16.0(0.0)	17.6(0.0)	23.0(0.0)	19.6(0.0)	19.7(0.0)	23.5(0.0)	4.9(0.2)	21.1(0.3)	6.9(0.1)	2.5(0.0)
105	17.8(3.3)	17.5(1.6)	20.0(1.3)	19.9(3.5)	18.4(1.1)	18.3(1.1)	12.5(1.8)	14.6(3.1)	18.7(2.4)	15.1(0.0)	14.0(1.7)	15.4(3.5)
113	0.4(0.0)	0.1(0.0)	0.7(0.0)	0.3(0.0)	9.6(0.0)	2.5(0.1)	21.5(0.1)	16.2(0.0)	4.0(0.0)	14.3(0.0)	14.1(0.0)	15.0(0.0)
173	0.0(0.0)	0.0(0.0)	0.1(0.1)	0.0(0.0)	0.0(0.0)	0.0(0.0)	0.0(0.0)	0.0(0.0)	0.0(0.0)	0.0(0.0)	0.0(0.0)	0.0(0.0)
177	2.1(2.1)	12.6(12.6)	0.5(0.5)	1.0(1.0)	25.8(25.6)	10.9(10.9)	8.8(8.8)	9.7(9.7)	1.1(1.1)	15.7(15.7)	1.6(1.6)	1.0(1.0)
243	33.2(0.6)	27.7(0.0)	34.1(0.0)	39.5(0.0)	/	/	/	/	/	/	/	/
271	16.8(0.0)	20.4(0.0)	1.0(0.0)	0.0(0.0)	23.4(0.0)	22.5(0.0)	22.7(0.0)	20.4(0.0)	0.0(0.0)	0.0(0.0)	0.0(0.0)	0.0(0.0)
284	0.0(0.0)	0.1(0.0)	0.0(0.0)	0.2(0.0)	0.0(0.0)	0.0(0.0)	0.0(0.0)	0.0(0.0)	0.0(0.0)	0.0(0.0)	0.0(0.0)	0.0(0.0)
285	/	/	/	/	0.3(0.0)	0.2(0.0)	0.4(0.0)	0.3(0.0)	0.2(0.0)	0.4(0.0)	0.0(0.0)	0.4(0.0)
370	/	/	/	/	18.7(2.1)	17.0(2.4)	14.1(3.3)	20.5(6.2)	8.8(0.9)	11.0(4.0)	5.7(0.1)	11.1(3.0)
373	3.7(0.0)	1.5(0.0)	4.0(0.0)	2.6(0.0)	2.8(0.0)	3.8(0.0)	3.7(0.0)	4.6(1.0)*	4.0(1.4)	3.4(0.0)	0.0(0.0)	2.0(0.0)

[†]This chain does not bind the cofactor.

[‡]In this chain, a different configuration of the nicotinamide ring and the protein loop 294-302, is observed.

[§]The ASA values are the average of two conformations.

Table S6. Secondary structure estimations for ADH1 and GSNOR before and after treatment with MMTS or H₂O₂ (for details see Experimental procedures). Percentage values derived from analysis of CD spectra with DichroWeb (CDSSTR/SP175 method) (<http://dichroweb.cryst.bbk.ac.uk/>).

Protein	Helix1	Helix1	Strand1	Strand1	Turn	Unordered	NRMSD
ADH1 (control)	5.3%	10.9%	22.1%	11.7%	12.2%	37.8%	0.024
ADH1 + 0.1 mM MMTS (2 h)	2.1%	7.1%	25.0%	13.1%	12.4%	40.4%	0.047
ADH1 + 2 mM H₂O₂ (2 h)	0.4%	7.3%	25.1%	13.6%	12.3%	41.2%	0.060
ADH1 + 2 mM H₂O₂ (4 h)	0.5%	6.9%	24.3%	13.0%	13.5%	41.7%	0.054
GSNOR (control)	6.6%	11.1%	21.6%	11.3%	12.6%	36.8%	0.026
GSNOR + 0.1 mM MMTS (1 h)	5.4%	10.4%	21.8%	11.7%	12.3%	38.3%	0.031
GSNOR + 2 mM H₂O₂ (2 h)	0.9%	6.8%	25.6%	13.4%	11.9%	41.4%	0.051
GSNOR + 2 mM H₂O₂ (4 h)	0.5%	6.3%	24.8%	13.2%	13.1%	42.1%	0.045

Table S7. Data collection and refinement statistics of ADHs structures.

	NADH-ADH1							Apo-GSNOR				
Data collection												
Unit cell (Å)	63.40	63.40	182.15	90.00	90.00	120.00		88.60	93.93	167.48	90.00	90.00
Space group				P3 ₁ 2						P2 ₁ 2 ₁ 2 ₁		
Resolution range* (Å)			182.15 – 1.70 (1.73 – 1.70)							81.92 – 1.90 (1.93 – 1.90)		
Unique reflections*			47829 (2492)							110542 (5434)		
Completeness* (%)			100.0 (100.0)							99.9 (100.0)		
R _{merge} *			0.068 (0.711)							0.136 (1.012)		
CC _{1/2} *			0.999 (0.827)							0.989 (0.739)		
I/σ(I) *			15.1 (2.3)							7.6 (1.8)		
Multiplicity*			8.5 (7.3)							5.4 (5.4)		
Refinement												
PDB ID	8CON							8CO4				
Resolution range* (Å)	47.02 – 1.70 (1.72 – 1.70)							81.92 – 1.90 (1.92 – 1.90)				
Reflection used	47747 (3104)							110373 (3701)				
R/R _{free}	0.186/0.214							0.161/0.211				
rmsd from ideality (Å, °)	0.006, 0.841							0.010, 1.045				
<i>N° atoms</i>												
Non-hydrogen atoms	3361							12745				
Protein atoms	2954							11550				
Zinc ions	2							8				
Cofactor atoms	44							/				
Solvent molecules	247							1040				
Hetero atoms	114							147				
<i>B</i> value (Å ²)												
Mean	31.8							26.6				
Wilson	24.1							22.2				
Protein atoms	30.6							25.7				
Zinc ions	23.5							/				
Cofactor atoms	31.6							34.2				
Solvent molecules	40.1							44.0				
Hetero atoms	44.6							44.0				
Ramachandran plot (%) [§]												
Most favoured	96.6							97.0				
Allowed	3.4							3.0				
Disallowed	0.0							0.0				